ACS SyntheticBiology

Research Article

pubs.acs.org/synthbio

Enhancing Bidirectional Electron Transfer of *Shewanella oneidensis* by a Synthetic Flavin Pathway

Yun Yang,[‡,§] Yuanzhao Ding,[§] Yidan Hu,[‡,§] Bin Cao,[§,∥] Scott A. Rice,[§] Staffan Kjelleberg,[§] and Hao Song*[,†]

[†]Key Laboratory of Systems Bioengineering (Ministry of Education), SynBio Research Platform, Collaborative Innovation Center of Chemical Science and Engineering (Tianjin), School of Chemical Engineering and Technology, Tianjin University, Tianjin 300072, P.R. China

[‡]School of Chemical and Biomedical Engineering, Nanyang Technological University, 70 Nanyang Drive, Singapore 637457, Singapore

[§]Singapore Centre on Environmental Life Sciences Engineering, Nanyang Technological University, 60 Nanyang Drive, Singapore 637551, Singapore

[∥]School of Civil and Environmental Engineering, Nanyang Technological University, 50 Nanyang Drive, Singapore 637798, Singapore

Supporting Information

ABSTRACT: Flavins regulate the rate and direction of extracellular electron transfer (EET) in *Shewanella oneidensis*. However, low concentration of endogenously secreted flavins by the wild-type *S. oneidensis* MR-1 limits its EET efficiency in bioelectrochemical systems (BES). Herein, a synthetic flavin biosynthesis pathway from *Bacillus subtilis* was heterologously expressed in *S. oneidensis* MR-1, resulting in ~25.7 times' increase in secreted flavin concentration. This synthetic flavin module enabled enhanced bidirectional EET rate of MR-1, in which its maximum power output in microbial fuel cells increased ~13.2 times (from 16.4 to 233.0 mW/m^2), and the inward current increased ~15.5 times (from 15.5 to 255.3 μA/cm^2).

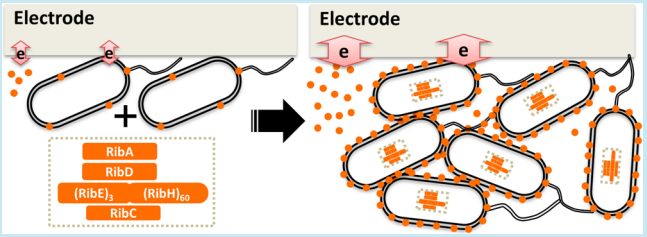

KEYWORDS: *extracellular electron transfer, flavin, cofactor, electron shuttle, synthetic biology, Shewanella oneidensis MR-1*

Extracellular electron transfer (EET) involves electron flow and exchange between intracellular and extracellular redox-active electron donors and acceptors. The kinetics and efficiency of EET are key factors in determining the performance of bioelectrochemical systems (BES), including microbial fuel cells (MFC), microbial electrolysis cells (MEC), and microbial electrosynthesis (MES), etc.[1,2] EET may occur bidirectionally, that is, outward EET in which electrons flow from cells to extracellular electron acceptors (such as anodes in MFC, and metal oxides for their reduction in biosynthesis of nanomaterials)[3−8] or inward EET in which electrons flow from cathodes into cells to generate intracellular reducing power for microbial electrosynthesis of chemicals.[9−11]

Shewanella oneidensis MR-1 has been extensively studied on its bidirectional electron flow across cell membranes.[12−16] Outward current flows from interior of cells to outer membrane (OM) and extracellular anodes through a metal-reducing conduit (Mtr pathway), where electrons (from NADH, the intracellular electron carrier) flow through the menaquinol pool, CymA (inner membrane [IM] tetraheme *c*-type cytochromes [*c*-Cyts]), MtrA (periplasmic decaheme *c*-Cyts), MtrB (β-barrel trans-OM protein) and finally to MtrC and OmcA (two OM decaheme *c*-Cyts) (Figure 1).[13,17−20] While the membrane conduit of OmcA-MtrCAB has been well established, the mechanism of interfacial electron extrange between OM *c*-Cyts and electrodes remains in dispute. One model of the interficial EET includes direct contact-based EET via OM *c*-Cyts or nanowires, and shuttle-mediated EET via endogenously secreted soluble flavins including flavin mononucleotide (FMN) and riboflavin (RF).[21−24] Reduced flavin carries the electrons from OM *c*-Cyts to the external electron acceptor (i.e., anode) by diffusion. After discharging electrons to anodes in a two-electron reaction mode, the oxidized flavin diffuses back and gets recharged by OM *c*-Cyts.[13,23,24] The electron shuttle flavin-mediated electron transfer was proven to dominate the EET of *S. oneidensis*.[25] Recently, another interfacial EET model was proposed, where flavin may serve as a cofactor binding to OmcA or MtrC to dictate EET.[26−29] Fully oxidized flavin (Ox) accepts one electron from reduced heme of OM *c*-Cyts, and binds to OM *c*-Cyts as a cofactor in the semiquinone (Sq) form with shifted potential. Ox/Sq redox cycling in OM *c*-Cyts donates electrons to electrodes in an one-electron reaction mode via direct contact. The OmcA-MtrCAB

Received: October 3, 2014
Published: January 26, 2015

DOI: 10.1021/sb500331x
ACS Synth. Biol. 2015, 4, 815−823

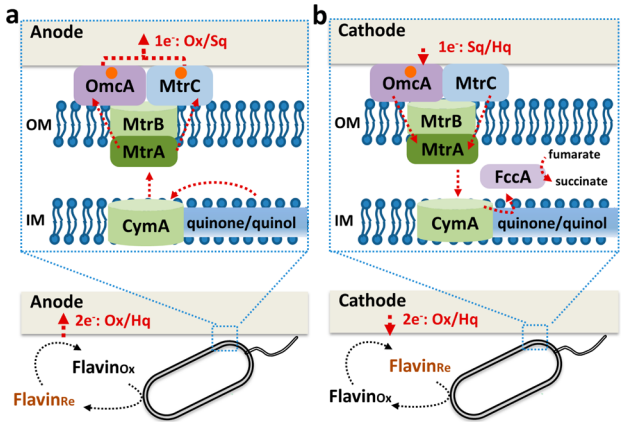

Figure 1. Schematic illustration of the flavin-mediated bidirectional extracellular electron transfer (EET) models of *Shewanella oneidensis*. Intracellular electrons flow through CymA and MtrA and come to OM *c*-Cyts (OmcA and MtrC). The interfacial electron transfer between OM and electrode interfaces may occur by direct contact-based EET, via OM *c*-Cyts or nanowires, or indirect EET mediated by flavins as electron shuttles. Ox/Hq cycling of free flavins dominants in this EET model. On the other hand, flavins may function as cofactors, and Ox/Sq cycling with positively shifted potential conducts outward electron flow (a), while Sq/Hq cycling with negatively shifted potential allows inward current (b). Filled orange circles represent flavin molecules in Sq form as cofactors.

conduit and interfacial EET pathways are reversible, which allows the occurrence of inward currents to cells from cathodes.[27,30,31] Especially, the Sq/Hq (fully reduced flavin) redox cycling with negatively shifted potential may account for inward EET in the proposed cofactor model (Figure 1).

Despite the controversies in the interfacial EET mechanisms of *Shewanella*, there is no doubt that flavins play fundamental roles in the interfacial EET, which is a rate-limiting step in the EET processes. However, the low concentration of naturally secreted flavins by the wild-type (WT) *S. oneidensis* MR-1 (~1 μM) limits its EET efficiency, especially the interfacial electron transfer from OM *c*-Cyts to electron acceptors. Diffusion of free flavin based on the Fick's diffusion law is a rate-limiting step for the shuttle-mediated EET. As the concentration gradient of either oxidized or reduced electron shuttle is determined by its total concentration, the low concentration of physiologically secreted flavins limits the shuttle-mediated EET.[2] In addition, in an assumed protein−ligand binding model for the flavin/OM *c*-Cyts interaction in the cofactor model,[26] the flavin dissociation constant of *S. oneidensis* was calculated to be over 10 μM, resulting in a small fraction of cofactor-occupied OM *c*-Cyts at the physiological flavin concentration of WT *S. oneidensis*. Thus, the concentration of flavins is a limiting factor for the efficient EET of *S. oneidensis*.

Although exogeneously added flavins could elevate the EET kinetics between OM *c*-Cyts and insoluble electron acceptors/donors,[25,28,32,33] the high cost of flavins as expensive additives would limit the large-scale BES applications. It is therefore of great significance to develop an engineered *S. oneidensis* strain with increased endogenous flavin production, avoiding the exogeneous addition of expensive flavins. To overcome the low concentration of secreted flavins in WT *S. oneidensis*, the synthetic biology approach, as a powerful and rational design strategy in engineering *S. oneidensis*,[34−36] was herein adopted to tune its bioelectrochemical performance.

In this work, a synthetic flavin synthesis pathway from *Bacillus subitlis* was heterologously expressed in *S. oneidensis* to increase the secreted flavin concentration, in order to strengthen the bidirectional electron conduits of *S. oneidensis*. *B. subtilis* is one of the most robust industrial riboflavin producers, and its flavin biosynthesis pathway is well studied.[37,38] Hence, the flavin synthesis pathway originated from *B. subtilis* was adapted and modularized for functionalization in *S. oneidensis* by our newly established standardized gene assembly tools in *S. oneidensis* (Supporting Information, Figure S1). In the synthetic flavin generation module (Figure 2a), flavin is synthesized from the precursors guanosine 5′-triphosphate (GTP) and D-ribulose 5′-phosphate (R5P). The flavin biosynthesis pathway includes GTP cyclohydrolase II/3,4-dihydroxy-2-butanone 4-phosphate synthase (RibA), a pyrimidine deaminase/reductase (RibD), a RF synthase (RibE), 6,7-dimethyl-8-ribityllumazine synthase (RibH), and a RF kinase/FMN adenylyltransferase (RibC). The intracellular produced flavin adenine dinucleotide (FAD) would be secreted into the periplasmic space by a native IM FAD transporter Bfe[25] and hydrolyzed to FMN by UshA (Figure 2c).[39] FMN diffuses out of cells through OM porins and is hydrolyzed gradually to form RF.

Such increased production of extracellular flavins boosted the rate of bidirectional EET in our engineered *S. oneidensis*. The outward EET was examined in MFCs, in which the maximum power output increased ~13.2 times from 16.4 to 233.0 mW/m^2. Meanwhile, the inward current density increased ~15.5 times from 15.5 to 255.3 μA/cm^2.

RESULTS AND DISCUSSION

Design of Standardized and Inducible Gene Expression Tools in *S. oneidensis*. Standardized molecular building blocks have been demonstrated to facilitate convenient and fast assembly of genetic modules;[40,41] such tools, however, have not been well established in *S. oneidensis*. To benefit the multigene assembly in *S. oneidensis*, a Biobrick compatible vector named pYYD (Supporting Information, Figure S1a) was constructed by replacing the original multiple cloning site (MCS) of pHG101 with a Biobrick specific restriction enzyme sites array (*Eco*RI, XbaI, SpeI, and SbfI). The array was flanked by terminators on both sides, insulating upstream and downstream transcriptional interference. An IPTG-inducible promoter element P*lacIq*-*lacIq*-P*tac* was introduced to form the expression vector pYYDT (Supporting Information, Figure S1b), allowing various gene expression levels upon differential IPTG induction.

Because of the codon usage bias between *S. oneidensis* and *B. subitlis*, *in vitro* synthesis of codon optimized genes instead of direct cloning from *B. subitlis* genome is necessary in order to prevent blocked translation due to shortage of tRNAs for rare codons. Each synthetic gene component of RibADEHC was modularly designed and *in vitro* synthesized, along with a RBS site, Biobrick prefix (*Eco*RI and XbaI), and suffix (SpeI and SbfI). The procedure is illustrated in Supporting Information Figure S2, and the primers for the gene syntheses are shown in Supporting Information Table S3. The flavin biosynthesis pathway was assembled by several routine Biobrick ligation steps. With an increased number of gene components in the flavin biosynthesis pathway being programmed, the constructed plasmids were named as pYYDT-C1, pYYDT-C2, pYYDT-C3, pYYDT-C4, pYYDT-C5, respectively, as illustrated in Figure

DOI: 10.1021/sb500331x
ACS Synth. Biol. 2015, 4, 815−823

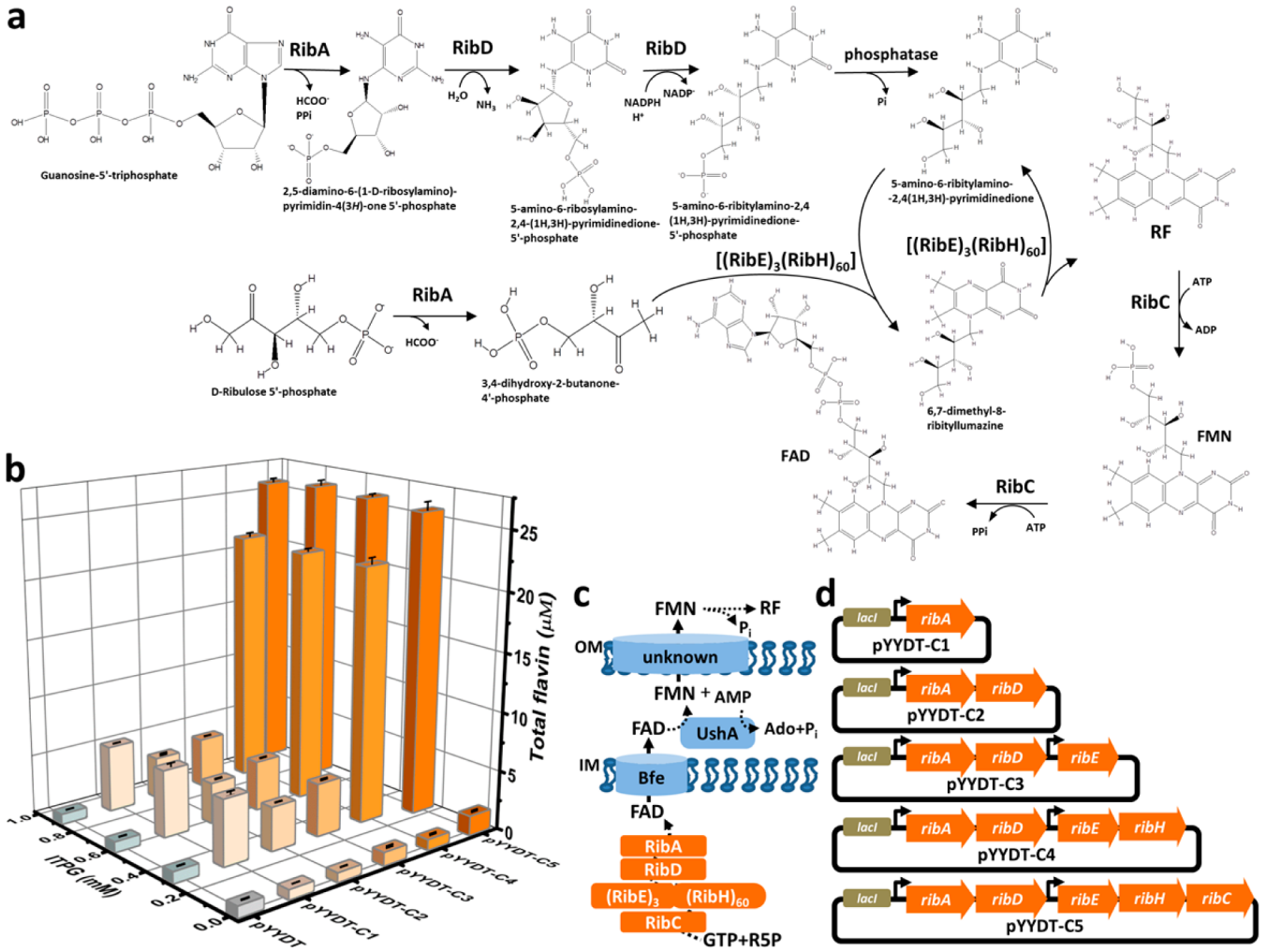

Figure 2. Construction of a synthetic flavin biosynthesis pathway in *S. oneidensis*. (a) Biosynthesis pathway of flavin in *Bacillus subtilis* and the functions of enzymes, which were heterologously cloned into *S. oneidensis*. FAD is synthesized from guanosine 5-triphosphate (GTP) and ribulose 5-phosphate (R5P) by the RibADEHC enzymes. (b) Flavin production concentration (μM, *z* axis) as a function of IPTG concentration (mM, *y* axis) by the recombinant *S. oneidensis* harboring various plasmids (*x*-axis showing the name of the harbored plasmid). The error bars showed standard deviations from independent triplicates. (c) Secretion pathway of the endogenously synthesized flavins by the engineered *S. oneidensis* strains. Cytoplasmic FAD is synthesized through synthetic flavin production module and is transported across IM through Bfe (bacterial FAD exporter). FAD in periplasm is transformed to FMN by the UshA enzyme. FMN diffuses across OM through an unknown porin and is hydrolyzed to RF. (d) Schematic plasmid maps of flavin expressing vectors. A constitutively expressed *lacI* gene was placed at the upstream of the flavin synthesis gene cluster. Two identical P*tac* promoters were utilized to drive coordinated expression of all the five genes for flavin synthesis.

2d. One additional P*tac* was placed after *ribD* to achieve coordinated efficient expression of all flavin synthetic genes.

Enhanced Production of Flavins by a Synthetic Flavin Pathway at Optimized Expression Level. The WT and each recombinant *S. oneidensis* strains were aerobically cultured at different IPTG induction levels, and the flavin concentrations secreted by these WT and mutant strains were measured by ultra-performance liquid chromatography (UPLC). After 10 h incubation, the flavin concentration was found to increase with the increased number of gene components in the flavin biosynthesis pathway (Figure 2b and d). The *S. oneidensis* strain (pYYDT-C5) bearing the entire flavin biosynthesis gene cluster *ribADEHC* could produce 26.15 ± 0.40 μM total flavins (20.80 ± 0.18 μM FMN, 5.36 ± 0.58 μM RF, n = 3) induced by 0.75 mM IPTG, which was ~25.7 times higher than that of the WT *S. oneidensis* (0.98 ± 0.03 μM total flavins, 0.91 ± 0.03 μM FMN, 0.08 ± 0.00 μM RF, n = 3). This demonstrated a successful construction of a functional synthetic flavin pathway in *S. oneidensis*.

We further found that the biosynthesis of flavins by the WT and the engineered *S. oneidensis* strain (pYYDT-C5) under anaerobic condition exhibited a similar trend but relatively lower levels than those under aerobic condition (see Supporting Information Table S2). The lower yield of flavins at anaerobic condition is mainly caused by the lower fluxes of the essential metabolic pathways for flavin biosynthesis (including gluconeogenesis pathway, pentose phosphate pathway [for R5P synthesis], and glycine pathway [glycine is the precursor of GTP]) at oxygen-limiting environment than those at aerobic condition.[42]

Enhanced Current Output in MFC. To assay the influence of increased endogenous flavins on EET exerted by the synthetic flavin pathway, the WT and recombinant *S. oeidensis* pYYDT-C5 were inoculated into an MFC anode with a 2 kΩ external resistor and recorded for voltage output,

DOI: 10.1021/sb500331x
ACS Synth. Biol. 2015, 4, 815−823

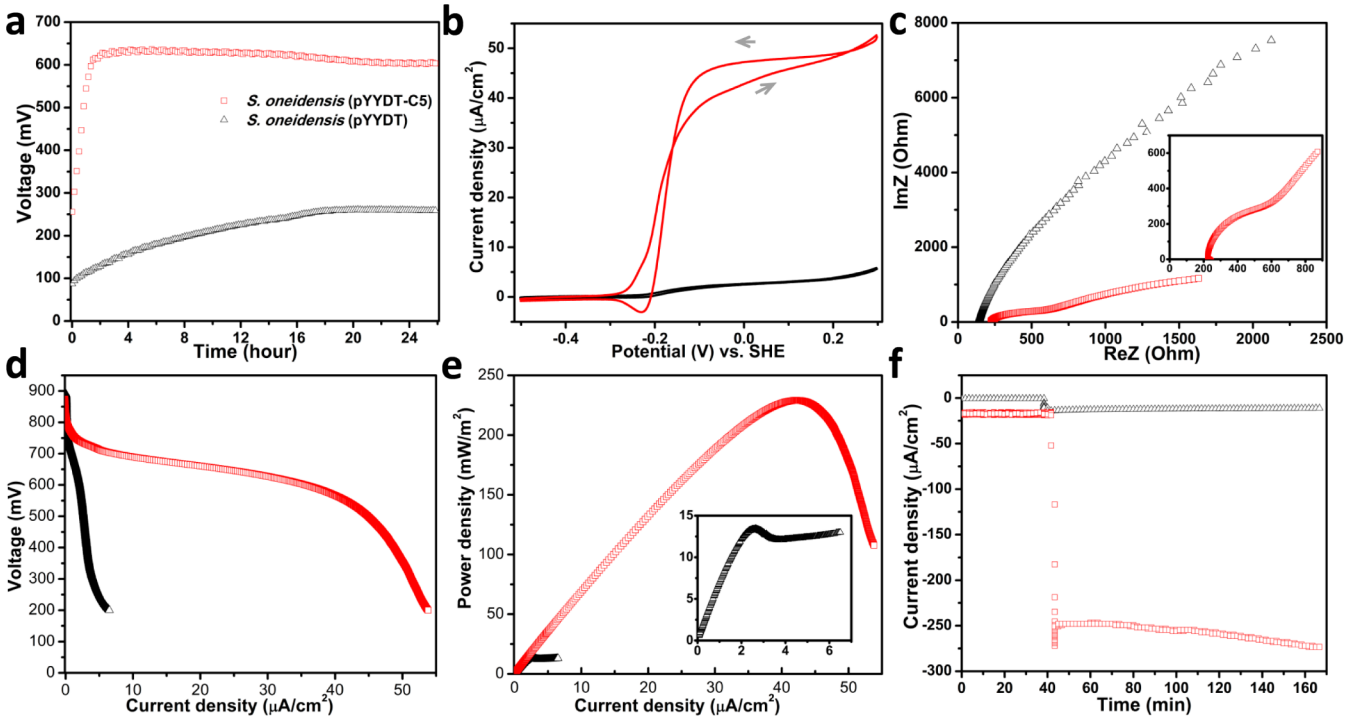

Figure 3. BES performance of the WT and the recombinant *S. oneidensis* harboring the pYYDT-C5 plasmid. (a) Voltage output of *S. oneidensis* harboring empty vector (black triangle) or flavin operon expressing vector (red square) in microbial fuel cells (MFCs). (b) Turnover cyclic voltammetry (CV) at a scan rate of 1 mV/s. (c) Nyquist plots of electrochemical impedance spectroscopy scanned at open circuit potential over 0.01−100 000 Hz with a 10 mV perturbation. (d) MFC polarization discharge curves obtained by linear sweep voltammetry (LSV) with a scan rate of 0.1 mV/s. (e) MFC power density output curves. (f) BES performance with a biocathode. The biocathode was poised at −0.36 V (vs SHE), and 50 mM fumarate was added at 42 min. The current density was normalized to the geometric electrode area.

respectively (Figure 3a). Upon connection of discharge circuit, the anodic current of the WT *S. oneidensis* rose in 24 h and reached the peak value of 269.9 ± 10.2 mV (n = 3). When the synthetic flavin pathway was introduced, the voltage generation by *S. oneidensis* pYYDT-C5 was much faster (rose rapidly in 2 h and reached peak voltage in 5 h), and reached a peak voltage of 634.0 ± 6.8 mV (n = 3). Thus, the presence of high-level flavins synthesized by the synthetic flavin module dramatically increased the voltage output.

EET Kinetics Revealed by Bioelectrochemistry Analysis. To investigate the underlying mechanism of enhanced EET, cyclic voltammetry (CV) at a low scan rate (allowing pseudosteady state redox reactions being established) was used to reveal redox reaction kinetics at cell−electrode interfaces. The CV for the WT and recombinant *S. oneidensis* pYYDT-C5 with and without synthetic flavin pathway are shown in Figure 3b. Upon the introduction of the synthetic flavin pathway, the well-defined free flavin redox peaks were greatly elevated originating from around −0.23 V (vs SHE). In addition, a higher potential window starting from around −0.1 V (vs SHE) occurred, corresponding to the OM *c*-Cyts. These results indicated the enhanced EET by overexpressed flavins was caused not only by the flavin-mediated electrode reduction but also via the OM *c*-Cyts-electrode contact-based pathway.

According to the Fick's diffusion law modified to reflect current density ($j = nF((D_{shuttle}\Delta C_{shuttle})/\Delta z)$, where $D_{shuttle}$ is the diffusion coefficient of electron shuttle, Δz is the transport distance, $\Delta C_{shuttle}$ is the concentration gradient of either oxidized or reduced shuttle, F is the Faraday's constant, and n is the number of moles of electrons transferred for oxidation of one mole of electron shuttle), the mediated current is mainly determined by the concentration gradient of electron shuttle.[2] The increased flavin concentration could increase the concentration gradient of either oxidized or reduced electron shuttles, accelerating the diffusion process of free flavin between cell−electrode interfaces. As diffusion process is a rate-limiting step of the shuttle-mediated EET, the increased flavin concentration could finally enhance the electron shuttle-mediated EET.

Additionally, it has been reported that exogeneously added flavins could increase biomass colonized on electrodes.[32] Hence, it is speculated that the elevated catalytic current via OM *c*-Cyts is due to more cells with the synthetic flavin module attached on the electrode. To further investigate the influence on direct EET exerted by the synthetic flavin module, the biofilm formation was assayed by confocal laser scanning microscopy imaging (CLSM). As shown in Figure 4, biofilm formation with the synthetic flavin module (Figure 4b) was thicker than that of the WT *S. oneidensis* (Figure 4a). Biofilm formation is a complex process, requiring swimming and swarming motilities via flagella, twitching motility via pili, and sliding motility via spreading by growth, *etc.*[43] Mutations in flagella or pili of *S. oneidensis* have shown impaired cell attachment or biofilm development.[44] The relevance of flavins in biofilm growth was previously put forward by proteomics studies, which showed that cells in biofilm upregulated RibB protein, a key enzyme of intrinsic flavin synthesis, as well as synthesis of GTP compared to planktonic cells.[45] Flavins could possibly promote biofilm formation through providing more energy via elevated Mtr respiration for the above-mentioned motilities and maintain the stability of the *S. oneidensis* biofilm.[46]

DOI: 10.1021/sb500331x
ACS Synth. Biol. 2015, 4, 815−823

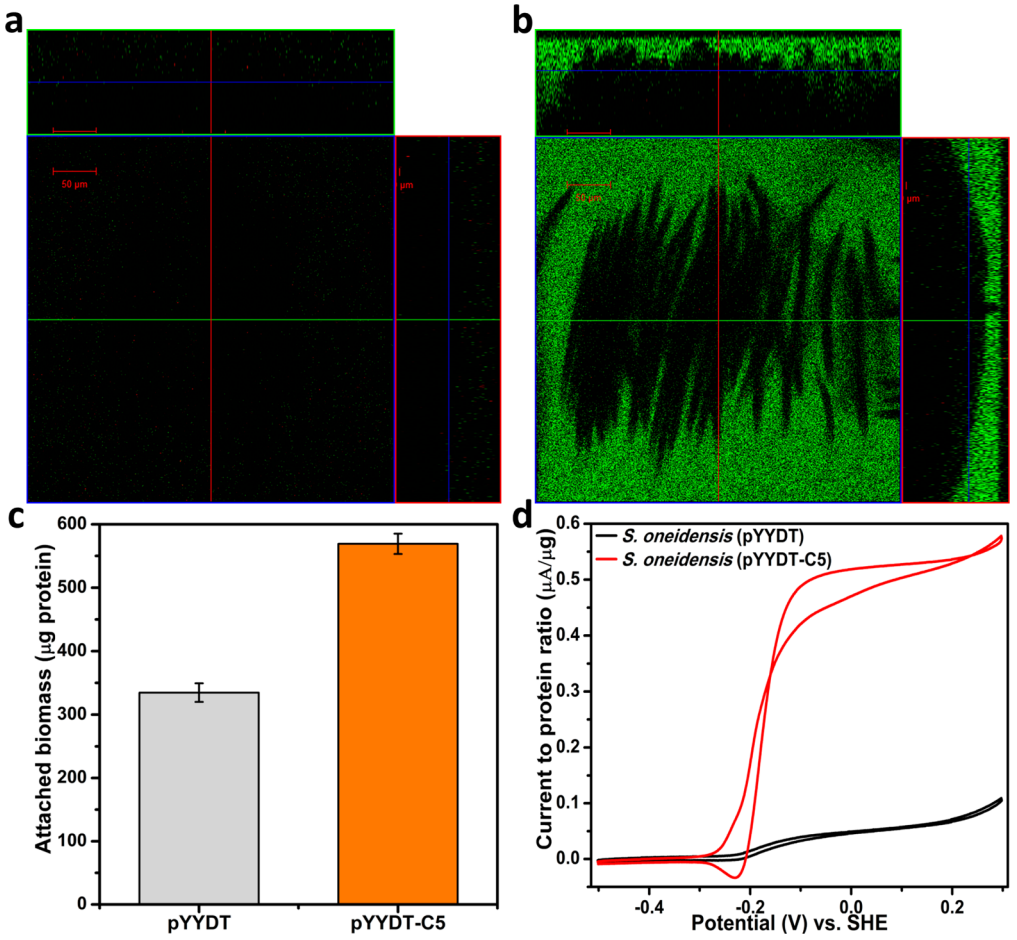

Figure 4. Confocal images of biofilms of the WT (a) and the recombinant *S. oneidensis* containing pYYDT-C5 (b) formed on the anodes of MFCs. The obvious dark radial pattern in b is the shape of carbon fibers from carbon cloth. Pictures were taken at three random spots on each electrode, and the representative image is shown here. The attached biomass of each strain on anodes was measured from three independent MFC anode chambers (c). Standardized CV curves normalized by the attached biomass on anodes (d).

To clarify whether the improved EET can be attributed to more attached cells or more electro-active cells, the CV signals were normalized to the colonized biomass on electrodes (Figure 4d). The recombinant *S. oneidensis* with the synthetic flavin module was measured to have 569.1 ± 16.0 μg protein (n = 3) attached on the electrodes, while the WT *S. oneidensis* had 334.6 ± 14.7 μg protein (n = 3) (see Figure 4c). The normalized CV showed higher EET rate of the recombinant *S. oneidensis* (Figure 4d). These results indicate that the overall elevated EET is due to not only more colonized cells on electrodes but also more bioelectroactivity of each cell enabled by the synthetic flavin pathway.

MFC Performance. To estimate the performance of MFC, linear sweep voltammetry (LSV) at a low scan rate (0.1 mV/s) was used to get the polarization curves (Figure 3d).[47,48] The dropping slope of polarization curves obtained from the recombinant *S. oneidensis* pYYDT-C5 was smaller than that obtained from the WT *S. oneidensis,* indicating less internal resistance in MFC. By multiplying the current with its corresponding voltage, the power density output curves could be calculated. The power density output curves (Figure 3e) showed that the recombinant *S. oneidensis* harboring pYYDT-C5 obtained a maximum power density of 233.0 ± 24.9 mW/m^2 (n = 3), which is ∼13.2 times higher than that of the WT *S. oneidensis* (16.4 ± 2.8 mW/m^2, n = 3) (the triplicates are shown in Supporting Information Figure S3).

Electrochemical impedance spectroscopy (EIS) was also performed to precisely evaluate the internal resistance of the MFCs inoculated with these *Shewanella* strains. By observing the diameter of the semicircle at medium-high frequency of the Nyquist plot (Figure 3c), the internal charge-transfer resistance was decreased from ∼3 kΩ of the WT *S. oneidensis* to ∼600 Ω of the recombinant *S. oneidensis* pYYDT-C5 containing the synthetic flavin pathway.

Enhanced Inward Current. Besides MFC performance associated with outward EET, inward current also benefited from the synthetic flavin pathway. The final electron acceptor of the well-established inward EET system in *Shewanella* is fumarate.[30] Upon addition of 50 mM fumarate, both strains (WT and recombinant *S. oneidensis*) showed a prompt onset of cathodic current (Figure 3f). The recombinant *S. oneidensis* pYYDT-C5 strain showed a significant increase in the inward current density (255.3 μA/cm^2), which is ∼15.5 times higher than that of the WT *S. oneidensis* (15.5 μA/cm^2).

In summary, a synthetic flavin synthesis pathway was constructed in *S. oneidensis*. It increased the endogenous production of flavins by ∼25.7 folds and consequently elevated both flavin-mediated and direct contact based EET. More attached cells and more electro-active cell on the electrodes were observed. The Mtr conduit strengthened by the synthetic flavin synthesis module is rapid and efficient, allowing BES applications related to inward and outward EET.

DOI: 10.1021/sb500331x
ACS Synth. Biol. 2015, 4, 815−823

METHODS

***In Vitro* Gene Synthesis.** *ribADEHC* genes of *B. subtilis* were identified, and their coding sequences were extracted from KEGG[49] and BioCyc database.[50] Each coding sequence was input into JCAT to adapt codon usage to express in *S. oneidensis*,[51] restriction enzyme sites of *Eco*RI, XbaI, SpeI, and SbfI were avoided in optimized sequences. Each final sequence to be *in vitro* synthesized is composed of one optimized coding sequence flanked by an upstream BBF RFC 20 prefix (containing *Eco*RI and XbaI), a RBS site (BBa_B0034, iGEM), a 6 bp random sequence and a downstream BBF RFC 20 suffix (containing SpeI and SbfI).[52,53]

To avoid high error rate when synthesize long fragment, each final sequence was divided into several building blocks (less than 750 bp) with overlaps performed by GeneDesign.[54,55] Oligonucleotide sets for PCR based gene assembly of each building block were designed by TmPrime.[56] Each assembled building block was ligated into peasyblunt vector (Transgen biotech, China) and sequenced (Genewiz, China). Correct building blocks belonging to one final sequence were ligated together via overlap PCR, cloned into peasyblunt vector, and sequenced. See Supporting Information Figure S2 (gene synthesis flowchart) and Table S3 (primer sequences).

Plasmid Construction and Transformation. All plasmid constructions were performed in *Escherichia coli* DH5α (DSM 6897). *E. coli* strains were cultured in LB medium at 37 °C with 200 rpm. Whenever needed, 50 μg/mL kanamycin was added in the culture medium.

A ~300 bp oligonucleotide was synthesized, containing a terminator stem loop, multicloning sites (including *Eco*RI, XbaI, SpeI, and SbfI), and a double terminator (BBa_B0015, iGEM). This fragment was flanked by two AgeI restriction sites at each end, and the original multicloning sites between two AgeI restriction sites of pHG101 were substituted;[57] then, the pYYD plasmid formed. Insertions of Biobrick designed fragments into pYYD plasmid were done according to previous procedures.[52,53,58] A *PlacIq-lacIq-Ptac* fragment was cloned from pMAL-c vector (New England Biolabs, U.S.A.) as an inducible promoter Biobrick and incorporated into pYYD so as to form pYYDT vector.

Synthesized *ribA*, *ribD*, *ribE*, *ribH*, and *ribC* Biobricks were incorporated into pYYDT sequentially and form the resulting expression plasmids pYYDT-C1, pYYDT-C2, pYYDT-C3, pYYDT-C4, and pYYDT-C5. An additional *Ptac* (BBa_K864400, iGEM) was added before *ribE* Biobrick in plasmids pYYDT-C3, pYYDT-C4, and pYYDT-C5 (Figure 2d).

Plasmids to be transformed into *S. oneidensis* were first transformed into the plasmid donor strain *E. coli* WM3064 (a dap auxotroph) and transferred into *S. oneidensis* by conjugation.[59] Whenever needed, 100 μg/mL 2,6-diaminopimelic acid (DAP) was added for the growth of *E. coli* WM3064.

Culture Condition for Flavin Production and Flavin Measurements. *S. oneidensis* MR-1 (ATCC 700550) from −80 °C freezer stock was inoculated into 20 mL LB broth shaking at 30 °C overnight aerobically. For the flavin synthesis at aerobic condition, 1.6 mL *S. oneidensis* culture suspension was inoculated into 40 mL *Shewanella* basal medium[32] with 15 mM lactate. After growing 10 h at 30 °C with 200 rpm, the culture broth was subjected to flavin measurements. For the flavin synthesis at anaerobic condition, 0.6 mL *S. oneidensis* (harboring pYYDT or pYYDT-C5) culture suspension was inoculated into 15 mL *Shewanella* basal medium (with 15 mM lactate and 30 mM sodium fumarate) in a sealed 15-mL test tube. The yields of flavins were assayed after 10 h of incubation at 30 °C.

All standard solutions and sample supernatants were filtered and assayed by a reverse-phase C18 column (10 cm × 2.1 mm, 5 μm, Ascentis) using the Prominence UPLC system (Shimadzu, Japan), which was equipped with two LC-20AD pumps and a SPD-M20A diode array detector. The mobile phase was composed of methanol and 0.05 M ammonium acetate (pH = 6.0). The chromatographic separations utilized a linear gradient from 25:75 to 70:30 v/v methanol/0.05 M ammonium acetate within 8 min, followed by isocratic 70:30 v/v to 11 min, and isocratic 25:75 v/v to 16 min at a flow rate of 0.2 mL/min at 30 °C with 20 μL injection volume. The ranges of concentration for standard solutions were 1 nM to 57 μM for FAD, 15 nM to 73 μM for FMN, and 26 nM to 131 μM for RF, respectively. The elution times were around 3.5 min for FAD, 4.6 min for FMN, and 6.1 min for RF, respectively. Flavin concentrations were calculated based on the signals at 267 nm.

BES Setup. Overnight *S. oneidensis* suspension was transferred to 420 mL *Shewanella* basal medium with 15 mM lactate in 1 L flasks. For *S. oneidensis* harboring the empty vector pYYDT or pYYDT-C5, the medium were both supplemented with 50 μg/mL kanamycin and 0.75 mM IPTG to ensure consistent culture condition. After 10 h growth at 30 °C with 200 rpm, the cell suspension concentration was adjusted to same level (OD_{600} value equals to 0.5) and dispersed into the bioanode of three H cell reactors (with a working volume of 140 mL) for parallel. The bioanodes were purged with nitrogen gas to exclude oxygen.

Carbon cloth (Gashub, Singapore) was used as the electrodes for both anode (2.5 cm × 2.5 cm, i.e., the geometric area is 6.25 cm^2) and cathode (2.5 cm × 3 cm). The Nafion 117 membrane (Gashub, Singapore) was used to separate the anode and cathode, which was pretreated as follows. First, it was boiled in 3% hydrogen peroxide for 0.5 h in water bath (80 °C). After being washed with distilled water several times, it was then boiled in distilled water for 0.5 h at 80 °C. Finally, it was boiled in 0.5 M sulfuric acid for 0.5 h at 80 °C, washed, and kept in sterile distilled water before H cell setup.[60] The cathodic electrolyte was made of 50 mM $K_3[Fe(CN)_6]$ in 50 mM KCl solution. A 2 kΩ external resistor was connected to both anode and cathode. MFC reactors were incubated at 30 °C, and the voltage outputs were continuously recorded by data acquisition cards MPS-110001 (Morpheus Electronics Technology Co. Ltd., China)

Procedures for BES setup with biocathode were similar, except that the cells were inoculated into cathode (carbon cloth: 2.5 cm × 2.5 cm), and anodic electrolyte (carbon cloth: 2.5 cm × 3 cm) was made of 50 mM $K_4[Fe(CN)_6]$ in 50 mM KCl solution. The cathodes were continuously stirred by a multipoint magnetic stirrer UM-12T (USUN, China) at room temperature. The biocathodes were imposed at −0.36 V (vs SHE) by a multichannel potentiostat CHI 1000C (CH Instruments, U.S.A.).

Electrochemical Analysis. Cyclic voltammetry (CV) was performed in a three-electrode configuration with an Ag/AgCl reference electrode (CH Instruments, U.S.A.) on a CHI 1000C multichannel potentiostat (CH Instruments, U.S.A.). CV scan rate was 1 mV/s in the range from −0.5 to 0.3 V (vs SHE).

Polarization curves were obtained by linear sweep voltammetry (LSV) decreasing the potential at a rate of −0.1 mV/s from OCP to −0.2 V controlled by CHI 1000C.[47,48]

DOI: 10.1021/sb500331x
ACS Synth. Biol. 2015, 4, 815−823

Electrochemical impedance spectroscopy (EIS) experiments were measured using a multichannel potentiostat Solartron 1470E (Solartron Analytical, U.S.A.) over the frequency range of 10^{-2} to 10^{5} Hz with 10 mV amplitude.

Confocal Image. Confocal images were captured using a Carl Zeiss Confocal Laser Scanning Microscopy (CLSM) LSM 780 with 34 channels and transmitted light-PMT equipped with an Axio observer inverted microscope and different objective lenses (20×/0.4 NA, 40×/0.6 NA, 40×/1.3 NA oil, 63×/1.4 NA oil, and 100×/1.4 NA oil). The biofilms associated with electrodes were stained with the LIVE/DEAD Baclight bacterial viability kit (Invitrogen, U.S.A.). Laser wavelengths of 488 and 561 nm were utilized for image. Images were processed using ZEN 2011 software.

Electrode Attached Biomass Measurement. The electrode was placed in a 50 mL tube containing 5 mL of 0.2 M NaOH, vortexed for 1 min, and then incubated in a water bath at 96 °C for 20 min to lyse cells. The extracts were cooled to room temperature and tested by bicinchoninic acid (BCA) protein assay kit (Sigma, U.S.A.).

■ ASSOCIATED CONTENT

Supporting Information

Additional information showing the plasmid maps of pYYD and pYYDT, primer sequences for *in vitro* gene synthesis. This material is available free of charge via the Internet at http://pubs.acs.org.

■ AUTHOR INFORMATION

Corresponding Author

*E-mail: hsong@tju.edu.cn.

Author Contributions

Y.Y. and H.S. designed the experiments; Y.Y., Y.D., and Y.H. performed the experiments; B.C., S.A.R., and S.K. helped to analyze the experimental data; Y.Y. and H.S. wrote the manuscript.

Notes

The authors declare no competing financial interest.

■ ACKNOWLEDGMENTS

This research was supported by the Chinese National High Technology Research and Development Program ("863" Program: 2012AA02A701), the National Basic Research Program of China ("973" Program: 2014CB745100), National Natural Science Foundation of China (NSFC 21376174), a grant from Singapore Centre on Environmental Life Sciences Engineering (SCELSE, NTU), and an AcRF Tier-2 grant (MOE2011-T2-2-035, Singapore). We thank Prof. Dianne Newman for providing *E. coli* WM3064, Prof. Haichun Gao for providing plasmid pHG101, Prof. Yinjin Yuan for gene synthesis, and Mr. Zhenquan Lin and Mr. Yifan Li for the genetics of *Bacillus subtilis*.

■ ABBREVIATIONS

EET, extracellular electron transfer; BES, bioelectrochemical system; MFC, microbial fuel cell; MEC, microbial electrolysis cell; MES, microbial electrosynthesis; FMN, flavin mononucleotide; RF, riboflavin; FAD, flavin adenine dinucleotide; OM, outer membrane; IM, inner membrane; Ox, fully oxidized; Sq, semiquinone; Hq, hydroquinone; WT, wild type; GTP, guanosine 5′-triphosphate; R5P, D-ribulose 5′-phosphate; MCS, multiple cloning site; IPTG, isopropyl β-D-1-thiogalactopyranoside; CV, cyclic voltammetry; LSV, linear sweep voltammetry; EIS, electrochemical impedance spectroscopy; OCP, open circuit potential

■ REFERENCES

(1) Yang, Y. G., Xu, M. Y., Guo, J., and Sun, G. P. (2012) Bacterial extracellular electron transfer in bioelectrochemical systems. *Process Biochem. 47*, 1707−1714.

(2) Torres, C. I., Marcus, A. K., Lee, H. S., Parameswaran, P., Krajmalnik-Brown, R., and Rittmann, B. E. (2010) A kinetic perspective on extracellular electron transfer by anode-respiring bacteria. *FEMS Microbiol. Rev. 34*, 3−17.

(3) Franks, A. E., and Nevin, K. P. (2010) Microbial fuel cells, a current review. *Energies 3*, 899−919.

(4) Rimboud, M., Pocaznoi, D., Erable, B., and Bergel, A. (2014) Electroanalysis of microbial anodes for bioelectrochemical systems: Basics, progress, and perspectives. *Phys. Chem. Chem. Phys. 16*, 16349−16366.

(5) Logan, B. E. (2009) Exoelectrogenic bacteria that power microbial fuel cells. *Nat. Rev. Microbiol. 7*, 375−381.

(6) Lovley, D. R. (2006) Bug juice: Harvesting electricity with microorganisms. *Nat. Rev. Microbiol. 4*, 497−508.

(7) Ng, C. K., Sivakumar, K., Liu, X., Madhaiyan, M., Ji, L. H., Yang, L., Tang, C. Y., Song, H., Kjelleberg, S., and Cao, B. (2013) Influence of outer membrane *c*-type cytochromes on particle size and activity of extracellular nanoparticles produced by *Shewanella oneidensis*. *Biotechnol. Bioeng. 110*, 1831−1837.

(8) Wang, V. B., Chua, S. L., Cao, B., Seviour, T., Nesatyy, V. J., Marsili, E., Kjelleberg, S., Givskov, M., Tolker-Nielsen, T., Song, H., Say, J., Loo, C., and Yang, L. (2013) Engineering PQS Biosynthesis pathway for enhancement of bioelectricity production in *Pseudomonas aeruginosa* microbial fuel cells. *PLoS One 8* (5), e63129.

(9) Rabaey, K., and Rozendal, R. A. (2010) Microbial electrosynthesis—Revisiting the electrical route for microbial production. *Nat. Rev. Microbiol. 8*, 706−716.

(10) Nevin, K. P., Woodard, T. L., Franks, A. E., Summers, Z. M., and Lovley, D. R. (2010) Microbial electrosynthesis: Feeding microbes electricity to convert carbon dioxide and water to multicarbon extracellular organic compounds. *MBio 1* (2), e00103−10.

(11) Lovley, D. R., and Nevin, K. P. (2013) Electrobiocommodities: Powering microbial production of fuels and commodity chemicals from carbon dioxide with electricity. *Curr. Opin. Biotechnol. 24*, 385−390.

(12) Jiao, Y., Qian, F., Li, Y., Wang, G., Saltikov, C. W., and Gralnick, J. A. (2011) Deciphering the electron transport pathway for graphene oxide reduction by *Shewanella oneidensis* MR-1. *J. Bacteriol. 193*, 3662−3665.

(13) Coursolle, D., Baron, D. B., Bond, D. R., and Gralnick, J. A. (2010) The Mtr respiratory pathway is essential for reducing flavins and electrodes in *Shewanella oneidensis*. *J. Bacteriol. 192*, 467−474.

(14) Bretschger, O., Obraztsova, A., Sturm, C. A., Chang, I. S., Gorby, Y. A., Reed, S. B., Culley, D. E., Reardon, C. L., Barua, S., Romine, M. F., Zhou, J., Beliaev, A. S., Bouhenni, R., Saffarini, D., Mansfeld, F., Kim, B. H., Fredrickson, J. K., and Nealson, K. H. (2007) Current production and metal oxide reduction by *Shewanella oneidensis* MR-1 wild type and mutants. *Appl. Environ. Microbiol. 73*, 7003−7012.

(15) Schuetz, B., Schicklberger, M., Kuermann, J., Spormann, A. M., and Gescher, J. (2009) Periplasmic electron transfer via the *c*-type cytochromes MtrA and FccA of *Shewanella oneidensis* MR-1. *Appl. Environ. Microb. 75*, 7789−7796.

(16) Lies, D. P., Hernandez, M. E., Kappler, A., Mielke, R. E., Gralnick, J. A., and Newman, D. K. (2005) *Shewanella oneidensis* MR-1 uses overlapping pathways for iron reduction at a distance and by direct contact under conditions relevant for biofilms. *Appl. Environ. Microb. 71*, 4414−4426.

(17) Coursolle, D., and Gralnick, J. A. (2012) Reconstruction of extracellular respiratory pathways for iron(III) reduction in *Shewanella*

DOI: 10.1021/sb500331x
ACS Synth. Biol. 2015, 4, 815−823

oneidensis strain MR-1. *Front. Microbiol. 3*, 56 DOI: 10.3389/fmicb.2012.00056.
(18) Gescher, J. S., Cordova, C. D., and Spormann, A. M. (2008) Dissimilatory iron reduction in *Escherichia coli*: Identification of CymA of *Shewanella oneidensis* and NapC of *E. coli* as ferric reductases. *Mol. Microbiol. 68*, 706−719.
(19) Okamoto, A., Hashimoto, K., and Nakamura, R. (2012) Long-range electron conduction of *Shewanella* biofilms mediated by outer membrane *c*-type cytochromes. *Bioelectrochemistry 85*, 61−65.
(20) Okamoto, A., Nakamura, R., and Hashimoto, K. (2011) *In vivo* identification of direct electron transfer from *Shewanella oneidensis* MR-1 to electrodes via outer-membrane OmcA-MtrCAB protein complexes. *Electrochim. Acta 56*, 5526−5531.
(21) El-Naggar, M. Y., Wanger, G., Leung, K. M., Yuzvinsky, T. D., Southam, G., Yang, J., Lau, W. M., Nealson, K. H., and Gorby, Y. A. (2010) Electrical transport along bacterial nanowires from *Shewanella oneidensis* MR-1. *Proc. Natl. Acad. Sci. U.S.A. 107*, 18127−18131.
(22) Brutinel, E. D., and Gralnick, J. A. (2012) Shuttling happens: Soluble flavin mediators of extracellular electron transfer in *Shewanella*. *Appl. Microbiol. Biot. 93*, 41−48.
(23) Marsili, E., Baron, D. B., Shikhare, I. D., Coursolle, D., Gralnick, J. A., and Bond, D. R. (2008) *Shewanella* secretes flavins that mediate extracellular electron transfer. *Proc. Natl. Acad. Sci. U.S.A. 105*, 3968−3973.
(24) von Canstein, H., Ogawa, J., Shimizu, S., and Lloyd, J. R. (2008) Secretion of flavins by *Shewanella* species and their role in extracellular electron transfer. *Appl. Environ. Microb. 74*, 615−623.
(25) Kotloski, N. J., and Gralnick, J. A. (2013) Flavin electron shuttles dominate extracellular electron transfer by *Shewanella oneidensis*. *MBio 4* (1), e00553−12.
(26) Okamoto, A., Nakamura, R., Nealson, K. H., and Hashimoto, K. (2014) Bound flavin model suggests similar electron-transfer mechanisms in *Shewanella* and *Geobacter*. *ChemElectroChem. 1*, 1808−1812 DOI: 10.1002/celc.201402151.
(27) Okamoto, A., Hashimoto, K., and Nealson, K. H. (2014) Flavin redox bifurcation as a mechanism for controlling the direction of electron flow during extracellular electron transfer. *Angew. Chem., Int. Ed. 53*, 10988−10991.
(28) Okamoto, A., Hashimoto, K., Nealson, K. H., and Nakamura, R. (2013) Rate enhancement of bacterial extracellular electron transport involves bound flavin semiquinones. *Proc. Natl. Acad. Sci. U.S.A. 110*, 7856−7861.
(29) Okamoto, A., Saito, K., Inoue, K., Nealson, K. H., Hashimoto, K., and Nakamura, R. (2014) Uptake of self-secreted flavins as bound cofactors for extracellular electron transfer in *Geobacter* species. *Energy Environ. Sci. 7*, 1357−1361.
(30) Ross, D. E., Flynn, J. M., Baron, D. B., Gralnick, J. A., and Bond, D. R. (2011) Towards Electrosynthesis in *Shewanella*: Energetics of Reversing the Mtr Pathway for Reductive Metabolism. *PLoS One 6* (2), e16649.
(31) Okamoto, A., Kalathil, S., Deng, X., Hashimoto, K., Nakamura, R., and Nealson, K. H. (2014) Cell-secreted flavins bound to membrane cytochromes dictate electron transfer reactions to surfaces with diverse charge and pH. *Sci. Rep. 4*, No. 5628, DOI: 10.1038/srep05628.
(32) Baron, D., LaBelle, E., Coursolle, D., Gralnick, J. A., and Bond, D. R. (2009) Electrochemical measurement of electron transfer kinetics by *Shewanella oneidensis* MR-1. *J. Biol. Chem. 284*, 28865−28873.
(33) Ross, D. E., Brantley, S. L., and Tien, M. (2009) Kinetic characterization of OmcA and MtrC, terminal reductases involved in respiratory electron transfer for dissimilatory iron reduction in *Shewanella oneidensis* MR-1. *Appl. Environ. Microbiol. 75*, 5218−5226.
(34) Johnson, E. T., Baron, D. B., Naranjo, B., Bond, D. R., Schmidt-Dannert, C., and Gralnick, J. A. (2010) Enhancement of survival and electricity production in an engineered bacterium by light-driven proton pumping. *Appl. Environ. Microbiol. 76*, 4123−4129.
(35) Flynn, J. M., Ross, D. E., Hunt, K. A., Bond, D. R., and Gralnick, J. A. (2010) Enabling unbalanced fermentations by using engineered electrode-interfaced bacteria. *MBio 1* (5), e00190−10.
(36) Kane, A. L., Bond, D. R., and Gralnick, J. A. (2013) Electrochemical analysis of *Shewanella oneidensis* engineered to bind gold electrodes. *ACS Synth. Biol. 2*, 93−101.
(37) Abbas, C. A., and Sibirny, A. A. (2011) Genetic control of biosynthesis and transport of riboflavin and flavin nucleotides and construction of robust biotechnological producers. *Microbiol. Mol. Biol. Rev. 75*, 321−360.
(38) Sauer, U., Cameron, D. C., and Bailey, J. E. (1998) Metabolic capacity of *Bacillus subtilis* for the production of purine nucleosides, riboflavin, and folic acid. *Biotechnol. Bioeng. 59*, 227−238.
(39) Covington, E. D., Gelbmann, C. B., Kotloski, N. J., and Gralnick, J. A. (2010) An essential role for UshA in processing of extracellular flavin electron shuttles by *Shewanella oneidensis*. *Mol. Microbiol. 78*, 519−532.
(40) Tsvetanova, B., Peng, L., Liang, X., Li, K., Yang, J. P., Ho, T., Shirley, J., Xu, L., Potter, J., Kudlicki, W., Peterson, T., and Katzen, F. (2011) Genetic assembly tools for synthetic biology. *Methods Enzymol. 498*, 327−348.
(41) Ellis, T., Adie, T., and Baldwin, G. S. (2011) DNA assembly for synthetic biology: From parts to pathways and beyond. *Integr. Biol. (Camb.) 3*, 109−118.
(42) Tang, Y. J. J., Hwang, J. S., Wemmer, D. E., and Keasling, J. D. (2007) *Shewanella oneidensis* MR-1 fluxome under various oxygen conditions. *Appl. Environ. Microb. 73*, 718−729.
(43) Kearns, D. B. (2010) A field guide to bacterial swarming motility. *Nat. Rev. Microbiol. 8*, 634−644.
(44) Thormann, K. M., Saville, R. M., Shukla, S., Pelletier, D. A., and Spormann, A. M. (2004) Initial phases of biofilm formation in *Shewanella oneidensis* MR-1. *J. Bacteriol. 186*, 8096−8104.
(45) De Vriendt, K., Theunissen, S., Carpentier, W., De Smet, L., Devreese, B., and Van Beeumen, J. (2005) Proteomics of *Shewanella oneidensis* MR-1 biofilm reveals differentially expressed proteins, including AggA and RibB. *Proteomics 5*, 1308−1316.
(46) Saville, R. M., Rakshe, S., Haagensen, J. A. J., Shukla, S., and Spormann, A. M. (2011) Energy-dependent stability of *Shewanella oneidensis* MR-1 biofilms. *J. Bacteriol. 193*, 3257−3264.
(47) Velasquez-Orta, S. B., Curtis, T. P., and Logan, B. E. (2009) Energy from algae using microbial fuel cells. *Biotechnol. Bioeng. 103*, 1068−1076.
(48) Zhao, F., Slade, R. C. T., and Varcoe, J. R. (2009) Techniques for the study and development of microbial fuel cells: An electrochemical perspective. *Chem. Soc. Rev. 38*, 1926−1939.
(49) Kanehisa, M., and Goto, S. (2000) KEGG: Kyoto Encyclopedia of genes and genomes. *Nucleic Acids Res. 28*, 27−30.
(50) Caspi, R., Altman, T., Billington, R., Dreher, K., Foerster, H., Fulcher, C. A., Holland, T. A., Keseler, I. M., Kothari, A., Kubo, A., Krummenacker, M., Latendresse, M., Mueller, L. A., Ong, Q., Paley, S., Subhraveti, P., Weaver, D. S., Weerasinghe, D., Zhang, P. F., and Karp, P. D. (2014) The MetaCyc database of metabolic pathways and enzymes and the BioCyc collection of pathway/genome databases. *Nucleic Acids Res. 42*, D459−D471.
(51) Grote, A., Hiller, K., Scheer, M., Munch, R., Nortemann, B., Hempel, D. C., and Jahn, D. (2005) JCat: A novel tool to adapt codon usage of a target gene to its potential expression host. *Nucleic Acids Res. 33*, W526−W531.
(52) Austin, C. (2009) Constraint Relaxation of RFC 10 for Assembling Standard Biological Parts. *MIT Synthetic Biology Working Group Technical Reports*; MIT Artificial Intelligence Laboratory, MIT Synthetic Biology Working Group, Cambridge, MA. Available online: http://dspace.mit.edu/handle/1721.1/44962.
(53) International Genetically Engineered Machines competition, http://igem.org.
(54) Richardson, S. M., Nunley, P. W., Yarrington, R. M., Boeke, J. D., and Bader, J. S. (2010) GeneDesign 3.0 is an updated synthetic biology toolkit. *Nucleic Acids Res. 38*, 2603−2606.

DOI: 10.1021/sb500331x
ACS Synth. Biol. 2015, 4, 815−823

(55) Hughes, R. A., Miklos, A. E., and Ellington, A. D. (2011) Gene synthesis: Methods and applications. *Methods Enzymol. 498*, 277−309.
(56) Bode, M., Khor, S., Ye, H. Y., Li, M. H., and Ying, J. Y. (2009) TmPrime: Fast, flexible oligonucleotide design software for gene synthesis. *Nucleic Acids Res. 37*, W214−W221.
(57) Wu, L., Wang, J. X., Tang, P., Chen, H. J., and Gao, H. C. (2011) Genetic and molecular characterization of flagellar assembly in *Shewanella oneidensis*. *PLoS One 6* (6), e21479.
(58) Knight T. F. (2003) Idempotent vector design for standard assembly of BioBricks. *MIT Synthetic Biology Working Group Technical Reports*; MIT Artificial Intelligence Laboratory, MIT Synthetic Biology Working Group, Cambridge, MA. Available online: http://dspace.mit.edu/handle/1721.1/21168.
(59) Saltikov, C. W., and Newman, D. K. (2003) Genetic identification of a respiratory arsenate reductase. *Proc. Natl. Acad. Sci. U.S.A. 100*, 10983−10988.
(60) Ghasemi, M., Daud, W. R. W., Ismail, M., Rahimnejad, M., Ismail, A. F., Leong, J. X., Miskan, M., and Ben Liew, K. (2013) Effect of pre-treatment and biofouling of proton exchange membrane on microbial fuel cell performance. *Int. J. Hydrogen Energy 38*, 5480−5484.

DOI: 10.1021/sb500331x
ACS Synth. Biol. 2015, 4, 815−823